# DEVELOPMENT AND GEOMETRIC VALIDATION OF ALUMINUM VACUUM CHAMBER PROTOTYPES FOR THE SPS-II STORAGE RING*

T. Phimsen[1,†], S. Boonsuya[1], S. Chitthaisong[1], W. Woranut[1], K. Trongklang[1], A. Kwankasem[1], S. Sumklang[1], O. Seegauncha[1], J. Sukain[1],
[1] Synchrotron Light Research Institute, Nakhon Ratchasima, Thailand

*Abstract*

The development of the Siam Photon Source II (SPS-II), a fourth-generation light source, represents a significant leap in Thailand's synchrotron infrastructure. A primary objective of the project is the establishment of domestic technical expertise and industrial capability for producing high-precision vacuum components. This paper details the manufacturing and geometric validation of two critical aluminum alloy prototypes: a straight-section chamber and a bending chamber.

Key technological advancements include the optimization of domestic aluminum extrusion processes to achieve ultra-high vacuum (UHV) surface requirements and the implementation of oil-less, ethanol-cooled CNC machining to eliminate hydrocarbon contamination while maintaining high precision. A comprehensive metrology framework, utilizing laser trackers and high-resolution profiling, was employed to characterize manufacturing-induced distortions. Results confirm that the integrated fabrication workflow, which combines specialized internal fixturing and multi-pass TIG welding, successfully maintains the stringent geometric tolerances required for the storage ring. This work validates the technical readiness of Thailand's industrial sector for the full-scale production of the SPS-II vacuum system.

## INTRODUCTION

The Siam Photon Source II (SPS-II) is a 3.0 GeV fourth-generation synchrotron light source currently under development at the Synchrotron Light Research Institute (SLRI) in Thailand. Formally approved in January 2025, the machine adopts a Double Triple Bend Achromat (DTBA) lattice with a total circumference of 327.6 m, distributed across 14 identical unit cells, and is designed to achieve a natural emittance of 0.96 nm·rad [1, 2]. Meeting the high-brightness performance goals of this lattice imposes exceptionally stringent requirements on the vacuum system, as the ultra-low emittance necessitates high-gradient quadrupole and sextupole magnets with small bore radii that reduce the available clearance between the chamber exterior and the magnet poles to the sub-millimeter level at the most constrained locations [2].

The SPS-II vacuum system design philosophy concentrates high-capacity pumping near photon absorbers, which are the dominant outgassing sources under synchrotron radiation [2, 3]. Three-dimensional Molflow+ simulations predict an operational average pressure of 1.1 $\times 10^{-9}$ mbar after 100 Ah of beam conditioning, satisfying the vacuum lifetime requirements of the storage ring [2]. The vacuum chambers are fabricated from aluminum alloys, A6061-T6 for arc section bending chambers and A6063-T5 for straight section extrusion profiles, selected for their favorable combination of low outgassing rate, high thermal conductivity, and machinability [2, 3].

## DESIGN SPECIFICATIONS AND ACCEPTANCE CRITERIA

The prototyping program addresses two components: the middle straight section and the VCB-4 bending chamber. The geometric tolerance criteria governing these chambers are derived from the magnet aperture constraints detailed in the lattice design. Specifically, a manufacturing tolerance of 0.3 mm per meter of functional length is specified for transverse deformations, while a limit of 1.0 mm per meter is set for longitudinal deformation. These criteria, along with vacuum integrity requirements, are summarized in Table 1.

Table 1: Prototype Deformation Acceptance Criteria

| Parameter | Specification |
|---|---|
| Transverse deformation | < 0.3 mm/m |
| Longitudinal deformation | < 1.0 mm/m |
| Magnet interface clearance | ≥ 0.5 mm |

## STRAIGHT CHAMBER FABRICATION AND VALIDATION

The final dummy chamber design, shown in Fig. 1, adopts a circular main body profile (62.71 mm ID) with integrated cooling channels. This geometry achieved an as-extruded internal surface roughness of $R_a$ 0.162–0.529 μm without requiring additional polishing, confirming that the domestic manufacturer had successfully internalized prior process improvements. To ensure the absence of surface contaminants that could compromise the ultimate pressure, all components underwent a standardized multi-stage chemical cleaning protocol prior to assembly. This process included alkaline etching to remove the native oxide layer, followed by deionized water rinsing, mixed acid passivation, and a final stage of ultrasonic cleaning. Welding was subsequently performed using a second-generation optimized fixture, developed through the iterative prototyping program [4], in a five-stage sequence designed to minimize accumulated thermal distortion: starting with taper-to-flange sub-assemblies and concluding with the final

† thanapong@slri.or.th

taper-end attachment. A dual-shielding argon gas system was strictly maintained to protect both the weld pool and the internal bore surface from atmospheric oxidation, ensuring that the internal surface finish remained within UHV specifications.

Following welding, dimensional inspection was conducted using a precision height gauge and digital calipers. The resulting vertical and horizontal deformation profiles are illustrated in Fig. 2 The vertical deformation rate of 0.24 mm/m and horizontal rate of 0.28 mm/m both satisfied the 0.3 mm/m specification. The mean longitudinal length measured was 1531.88 mm, well within the ±1 mm budget. All geometric and integrity results for this prototype are consolidated in Table 2.

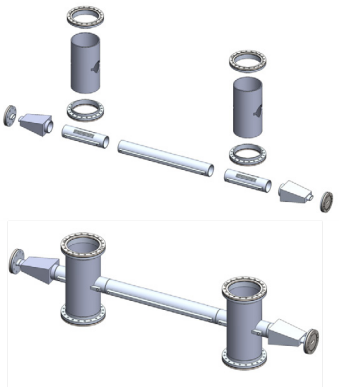

Figure 1: Exploded view of the middle straight dummy chamber assembly showing all major components.

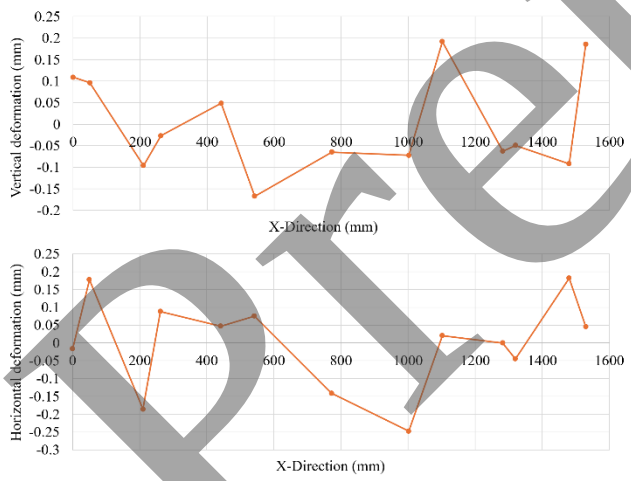


Figure 2: Measured vertical (top) and horizontal (bottom) deformation profiles along the dummy chamber longitudinal axis.

Table 2: Geometric Validation Results For The Middle Straight Dummy Chamber

| Deformation | Specification | Measured |
|---|---|---|
| Vertical (mm/m) | < 0.3 | 0.24 |
| Horizontal (mm/m) | < 0.3 | 0.28 |
| Longitudinal (mm) | < 1.0 | 0.88 |
| Flange parallelism (mrad) | - | 2.45 |

## BENDING CHAMBER FABRICATION AND VALIDATION

The VCB-4 bending chamber represents the most significant manufacturing challenge in the arc section due to its complex three-dimensional curved trajectory. Unlike the straight-section chambers, the VCB-4 must be fabricated from solid A6061-T6 aluminum billets using five-axis CNC machining, as extrusion is not technically feasible for its intricate internal profile. To eliminate hydrocarbon contamination at the source and avoid extensive post-machining remediation, all primary CNC operations were conducted using pure ethanol as the sole cutting fluid. This methodology, adapted from practices developed at the National Synchrotron Radiation Research Center (NSRRC) in Taiwan [5], was performed in a dedicated temporary cleanroom facility.

A custom ethanol spray cooling system, as illustrated in Fig. 3, was integrated with the five-axis machine to deliver the coolant through high-pressure nozzles equipped with inline filtration to prevent oil ingress. The measured dew point in the ethanol stream was recorded at –120°C, which significantly exceeds the –80°C requirement and confirms a machining environment free of both hydrocarbon and moisture contamination. Post-machining inspection confirmed an internal beam duct surface roughness of $R_a$ 0.08 µm, satisfying UHV cleanliness requirements and providing optimal conditions for subsequent TIG welding.

Figure 3: Ethanol spray cooling system installed at N.K.R. Engineering Company for oil-free five-axis CNC machining of the VCB-4 chamber halves.

Following standardized chemical cleaning, the VCB-4 components were assembled via an eight-stage TIG welding sequence. A critical process feature employed for this prototype was the use of pre-heating; heating elements were installed on the external surfaces to raise the structure to 80°C before seam welding commenced. This pre-heat phase is essential to reduce thermal gradients, slow the post-weld cooling rate, and suppress the accumulation of residual stresses, which is of particular importance for the large-aspect-ratio curved geometry of the VCB-4. Longitudinal seam welding was performed in segments with pauses for temperature equilibration. The final helium leak

rate was measured at $6.5 \times 10^{-11}$ mbar·L/s confirming the success of the welding operations.

Geometric characterization of the completed chamber was conducted using two complementary measurement systems: a Leica Absolute Tracker laser interferometer for 3D global coordinates at eight precision fiducial holes and a precision height gauge for a 28-point high-density vertical survey. Quantitative analysis utilized Singular Value Decomposition (SVD) for optimal reference plane fitting, where the resulting Root Mean Square Error (RMSE) served as a flatness metric. Furthermore, the Kabsch algorithm was applied for optimal rigid-body alignment between the measured and design coordinate sets. Residual displacement vectors calculated after this alignment represent genuine manufacturing deviations and serve as the primary compliance metric.

The laser tracker results, after Kabsch alignment, show that the vertical component dominates the deformation field, with the Outside Dipole section exhibiting systematic upward residuals. This behavior is visualized in the 2D deformation heatmap shown in Fig. 4. The high-density height gauge survey corroborated these findings and additionally resolved a torsional deformation mode, a transverse gradient of 0.240 mm, arising from asymmetric thermal stress relaxation during welding. This complex deformation is visualized in Fig. 5.

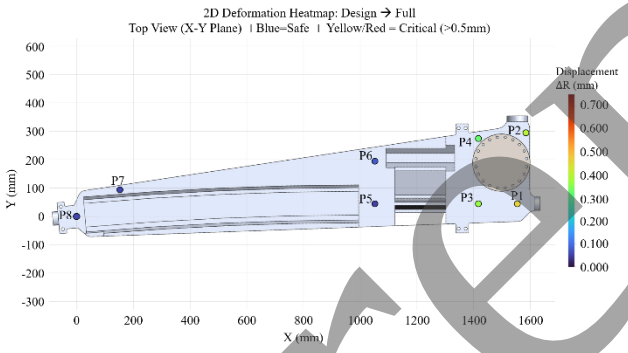


Figure 4: Vertical deformation heatmap from laser tracker.

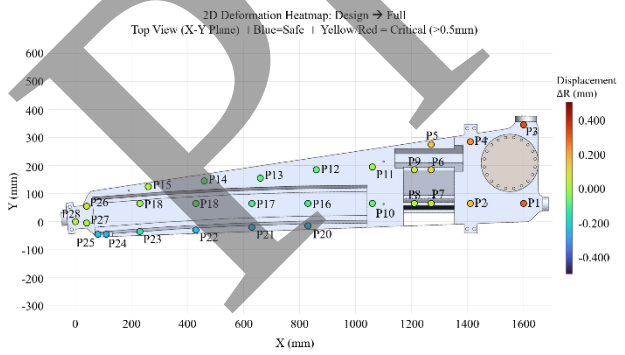


Figure 5: Vertical deformation heatmap from Height gauge measurement.

Despite these systematic modes, all measurements confirmed compliance with the ±0.255 mm bilateral tolerance envelope across all axes. Clearance verification at 23 magnetic interface positions yielded vertical deformations ranging from –0.101 mm to +0.092 mm. Against the minimum design radial clearance of 0.5 mm, the maximum observed deformation retains a safety factor exceeding 4:1, ensuring that the structural behavior does not compromise installation or operational safety. These results validate the oil-free machining and pre-heated welding workflow as a production-ready methodology for UHV bending chambers.

## DISCUSSION

The experimental data reveals that deformation mechanisms differ fundamentally between the two chamber architectures. In the straight-section chambers, the observed deviations arise primarily from accumulated dimensional variations at the machined mating surfaces, suggesting that tighter CNC tolerancing for interface geometries is the most direct path to increasing the current 7% horizontal deformation margin. Conversely, the VCB-4 bending chamber's deformation is dominated by the release of residual machining stresses during the welding thermal cycle, producing the characteristic inter-sectional bowing and torsional twist observed in the metrology data.

The dual-modality metrology approach—combining global laser tracker registration with high-density height gauge profiling—was essential for validating the VCB-4. The 31 µm agreement between these two independent datasets provides high confidence in the compliance assessment. Furthermore, the successful implementation of the oil-free ethanol machining process, which achieved a coolant dew point of –120°C, confirms that Thailand's domestic sector can now produce UHV-ready components without the hydrocarbon contamination risks associated with traditional oil-cooled machining.

## CONCLUSION

The fabrication and validation of these two prototypes demonstrate that the technical capability for full-scale SPS-II vacuum production has been successfully established within Thailand’s domestic industrial sector. Both the middle straight dummy chamber and the VCB-4 bending chamber achieved full compliance with the acceptance criteria derived from the DTBA lattice magnet aperture constraints. Specifically, the transverse deformations were maintained within the 0.3 mm/m limit, and helium leak rates remained significantly below the threshold. With the manufacturing workflow now qualified and documented, production of the straight-section chambers is authorized to proceed immediately. Bending chamber production will follow, with a specific focus on optimizing CNC tool paths to minimize subsurface stress accumulation, thereby targeting even greater geometric margins in the final production run. These results provide the technical foundation required for the successful assembly and operation of the SPS-II storage ring.

## REFERENCES


[1] P. Sudmuang *et al.*, “SPS-II project: Status update”, in *Proc. IPAC'25*, Taipei, Taiwan, Jun. 2025, pp. 903-908. doi:10.18429/JACoW-IPAC2025-TUZD2

[2] T. Phimsen *et al.*, “Vacuum system design and simulation for Siam Photon Source II: Towards Thailand's fourth-generation synchrotron light source”, in *Vacuum,* vol. 240, p. 114569, 2025.doi:10.1016/j.vacuum.2025.114569.

[3] T. Phimsen *et al.*, “Progress in vacuum system design for Thailand's new light source”, in *Vacuum,* vol. 234, p. 114111, 2025. doi: 10.1016/j.vacuum.2025.114111

[4] T. Phimsen *et al.*, “Fabrication challenges and lessons learned in prototyping SPS-II straight section vacuum chambers”, in *Proc. 13th Int. Conf. Mech. Eng. Design Synchrotron Radiat. Equip. Instrum. (MEDSI'25)*, Lund, Sweden. doi:10.18429/JACoW-MEDSI2025-WEP22

[5] G.-Y. Hsiung *et al.*, “TPS Vacuum System”, in *Proc. PAC'09*, Vancouver, Canada, May 2009, paper MO6RFP018, pp. 387-389.